International Journal of Mechanical Engineering and Applications
2023; 11(2): 38-48
http://www.sciencepublishinggroup.com/j/ijmea
doi: 10.11648/j.ijmea.20231102.11
ISSN: 2330-023X (Print); ISSN: 2330-0248 (Online)

Development of a Cubic Core Lightweight Panel Using Origami-Kirigami Engineering

Zhilei Tian[1], Jingchao Guan[1], Wei Zhao[2], Apollo B. Fukuchi[1], Xilu Zhao[1,*], Ichiro Hagiwara[3]

[1]Department of Mechanical Engineering, Saitama Institute of Technology, Saitama, Japan

[2]Space C5 Co., Ltd., Tokyo, Japan

[3]Institute for Advanced Study of Mathematical Sciences, Meiji University, Tokyo, Japan

Email address:

tzl880108@gmail.com (Zhilei Tian), guanjingchao123@gmail.com (Jingchao Guan), shunsuke0390@gmail.com (Wei Zhao), apollo-fukuchi@sit.ac.jp (Apollo B. Fukuchi), ihagi@meiji.ac.jp (Ichiro Hagiwara)

[*]Corresponding author

To cite this article:

Zhilei Tian, Jingchao Guan, Wei Zhao, Apollo B. Fukuchi, Xilu Zhao, Ichiro Hagiwara. Development of a Cubic Core Lightweight Panel Using Origami-Kirigami Engineering. *International Journal of Mechanical Engineering and Applications*. Vol. 11, No. 2, 2023, pp. 38-48. doi: 10.11648/j.ijmea.20231102.11

Received: February 2, 2023; **Accepted**: February 21, 2023; **Published**: March 21, 2023

Abstract: Honeycomb core panels are commonly used in industry as lightweight structures. However, because the bond between the face plate and the regular hexagonal core is weak, there are strength problems, such as heat and shear loads. In this study, a new cubic core panel was developed as an alternative to a honeycomb core panel. Unlike conventional honeycomb core panels, cubic cores can be processed from a single flat plate by punching and bending. Through the square contact area between the face plate and the cubic core, a double-bond integral panel structure was assembled using glue and rebates. The cubic core panel had a higher bending stiffness and bonding strength than the conventional honeycomb panel. A three-point bending test was performed on the processed cubic core panel. The relationship between the bending load and the deformation of the cubic core panel was determined. The curved part of the cubic core panel can be easily processed by cutting out a part of the material on one side of the cubic core panel in accordance with the lightweight structure of the curved part. A design formula for the curved part of the cubic core panel was derived using the curvature radius and curvature angle of the actual curved structure. A cubic core molding system was investigated using the parallel movement characteristics of the four-bar link mechanism for future mass production. An important design factor for practical use was obtained by deriving the relational expression between the bending load and plastic displacement.

Keywords: Origami Engineering, Kirigami Engineering, Lightweight Panel Structure, Honeycomb Core Panel, High-Stiffness Structure, Four-Link Mechanisms

1. Introduction

The development of lightweight structures against the backdrop of global energy problems is an important research topic in such industries as automobiles, aircraft, and machine tools [1–3]. To achieve this goal, the optimal design for structural weight reduction has been studied under conditions that satisfy mechanical performance [4–6]. In addition, lightweight structures using aluminum alloys and composite materials instead of ordinary metal materials are being studied [7–11].

Sandwich lightweight panels play an important role among the lightweight structures used in modern industry [12–15]. Among them, honeycomb core panels are the most widely used owing to their excellent specific strength and specific stiffness per weight [16–19]. In addition, the mechanical properties of honeycomb core panels under various conditions have been studied in detail. Stiffness and strength problems of honeycomb core panels in the presence of complex loads, such as dynamic and impact, have been investigated [20–22]. Because the honeycomb core panel is composed of thin plates, the problem of buckling under the compressive load has also been investigated [23–25]. Problems of stress concentration and fracture caused by

microdefects in materials and production processes have also been investigated [26–28]. Furthermore, the optimization of the shape parameters of the honeycomb core panel was investigated [29, 30]. These research results provide basic technical results useful for the practical development of honeycomb core panels.

However, the honeycomb core panel has the drawback of being difficult to apply to shear loads and thermal environments because the regular hexagonal core material and the face plate are bonded with glue through only the line-shaped contact area. There is also a processing problem for honeycomb core panels [31, 32].

Therefore, to improve the drawbacks of honeycomb core panels, which are used in large quantities in industry, it is important to promote research and development on new lightweight panels that can be processed by simpler methods and have good mechanical properties. Furthermore, such research is expected to have significant economic value.

In this article, a new cubic core panel is proposed instead of a conventional honeycomb core panel. A cubic core can be processed from a single flat metal plate by simple punching of a square hole and bending. In addition, glues and rebates can be used to assemble integral cubic core panels with double bonding through square contact surfaces between the faceplate and the cubic core. For investigation, a cubic core panel was created using an aluminum plate, and the mechanical properties of the cubic core panel were examined in a three-point bending test. The finite-element method (FEM) was used to analyze and compare the bending stiffness of the honeycomb core panel and that of the cubic core panel under the same numerical analysis conditions. Furthermore, for practical development, a processing method for a curved cubic core panel that is applied to the corner part of an actual vehicle structure was devised and investigated. A dedicated cubic core manufacturing system using a four-bar linkage mechanism was developed and examined for future mass production.

2. Materials and Methods

2.1. Cubic Core Panel

Figure 1 shows a conventional honeycomb core panel. As shown in Figure 1, the honeycomb core and face plate are bonded with glue. Because the bonding surface is in the form of a thin line, the bonding strength at this portion is relatively weak.

In this study, the cubic core shown in Figure 2 was employed instead of the conventional honeycomb core by making use of the knowledge obtained from origami and kirigami engineering [33, 34]. As shown in Figure 2, first, on a flat plate, square holes are drilled in every other horizontal and vertical direction. The sides of each square are then alternately folded up and down to obtain a cubic core. Finally, the cubic core panel is obtained by gluing the face plates to the upper and lower sides of the cubic core with glue and fixing the face plate and cubic core to the central point with rivets.

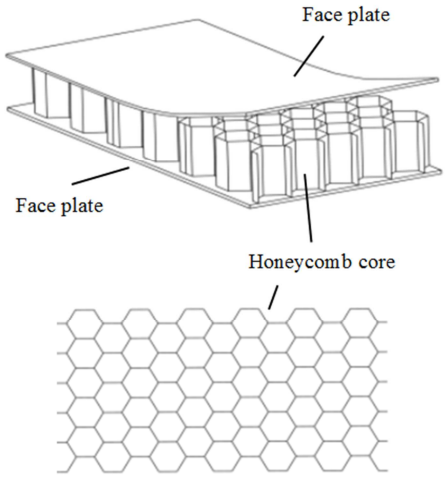

Figure 1. *Diagram of honeycomb core panel structure.*

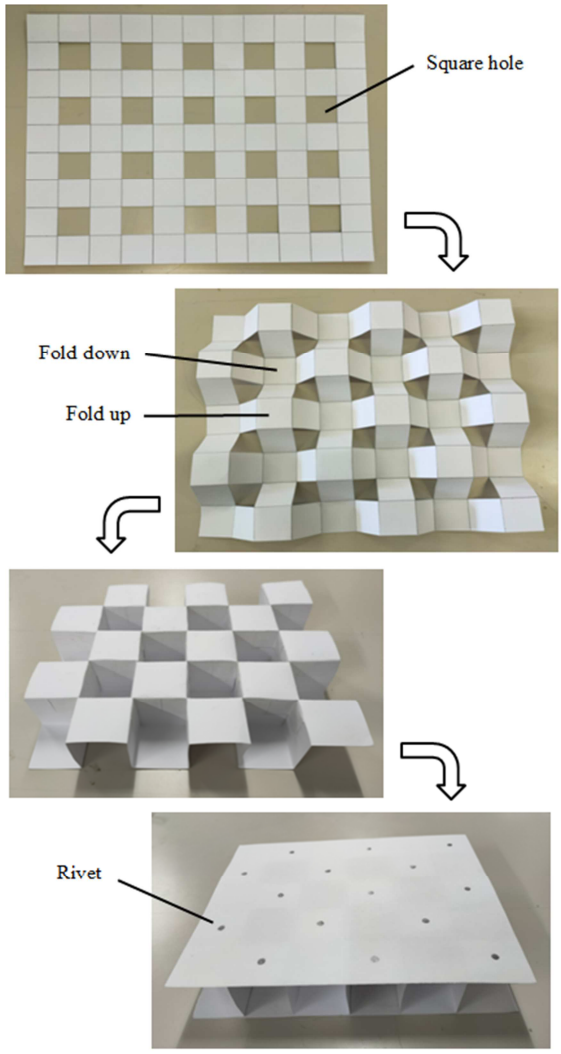

Figure 2. *Diagram of the cubic core panel configuration process.*

2.2. Comparison of Cubic and Honeycomb Core Panels

Figure 3 shows the simplified I-shaped equivalent cross section of a honeycomb panel and a cubic core panel with the same dimensions. The plate thickness t is assumed to be the

same for the face plate and the plate composing the core. As indicated by the red dotted line in the figure, the number *n* of vertical walls on both sides is the same; therefore, the central width of both I-shaped equivalent sections is the same *nt*. The thickness of the face plate of the I-shaped equivalent section of the honeycomb panel is *t*, and the thickness of the face plate of the I-shaped equivalent section of the cubic core can be approximated as 1.5*t*. Therefore, the equivalent moment of inertia of the honeycomb and cubic core panels and their difference can be calculated by the following equations.

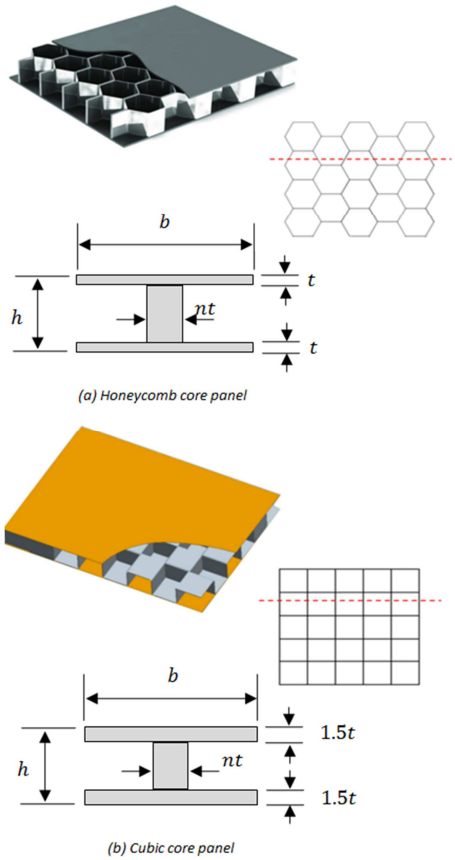

Figure 3. *Equivalent cross section of honeycomb and cubic core panel.*

$$I_{honey} = \frac{bh^3-(b-nt)(h-2t)^3}{12} \quad (1)$$

$$I_{cubic} = \frac{bh^3-(b-nt)(h-3t)^3}{12} \quad (2)$$

$$\Delta I = I_{cubic} - I_{hobey} = \frac{b-nt}{12}[(h-2t)^3 - (h-3t)^3] \quad (3)$$

In Equation (3), $b - nt > 0$ and $h - 2t > h - 3t$, so the following equation is obtained.

$$I_{cubic} > I_{hobey} \quad (4)$$

Equation (4) indicates that the cubic core panel has a higher bending stiffness than the honeycomb panel. However, as shown in Figure 3, the thickness of the equivalent face plate of the cubic core panel is larger than that of the honeycomb panel, and the weight is likely to be heavier. Therefore, it is necessary to evaluate the bending stiffness per unit weight of the panel.

If the materials of the two panels are the same, the material volume should be used for evaluation. From Figure 3, the material volume of the honeycomb panel and the cubic core panel can be calculated by

$$V_{honey} = b[bh - (b-nt)(h-2t) + (n-1)(h-2t)] \quad (5)$$

$$V_{cubic} = b[bh - (b-nt)(h-3t) + (n-1)(h-3t)] \quad (6)$$

Using the honeycomb panel as a comparison standard, the ratio of the geometrical moment of inertia and the material volume of the cubic core panel compared with the honeycomb panel can be summarized by using Equations (1), (2), (4), and (5). Figure 4 shows the comparison results. The horizontal axis in Figure 4 represents the width-to-thickness ratio h/b of the lightweight panel. However, the plate thickness is 1.0 mm, and the number of cores in the cubic and honeycomb core panels is the same.

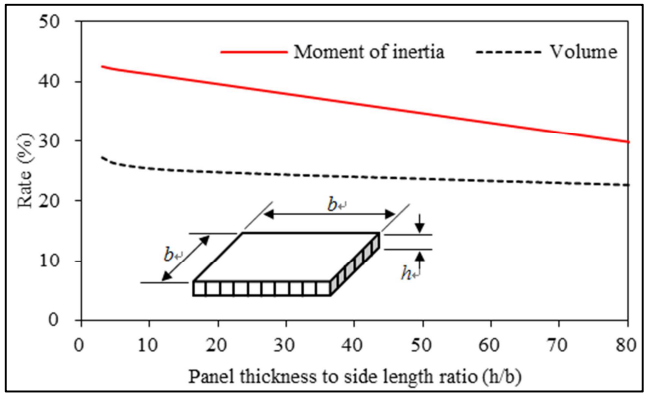

Figure 4. *Comparison of bending properties of honeycomb core panel and cubic core panel.*

Figure 4 reveals that the increase in the geometric moment of inertia is greater than the increase in the material volume when cubic core panels are used instead of honeycomb panels.

2.3. Manufacturing Test of Cubic Core Panel

A prototype cubic core panel was fabricated according to the procedure shown in Figure 5. The plate material used was aluminum A5052 with a thickness of 0.8 mm. First, as shown in Figure 5(a), a 450mm×300mm aluminum flat plate was cut using a laser to cut square holes with a side length of 30 mm at intervals of 30 mm horizontally and vertically. To bend it vertically, as shown in Figure 5 (b), wooden blocks were attached to the upper and lower sides of the flat plate part at equal intervals, and rubber rings were attached to the end faces of the wooden blocks so that they could slide easily. Then, as shown in Figure 5 (c), a pressing machine applied forming pressure to the flat plate part, the forming block slid horizontally while moving vertically, and the flat plate was bent, as shown in Figure 5 (d). The forming work was gradually divided into several steps, and, finally, the cubic core shown in Figure 5 (e) was obtained through hand finishing.

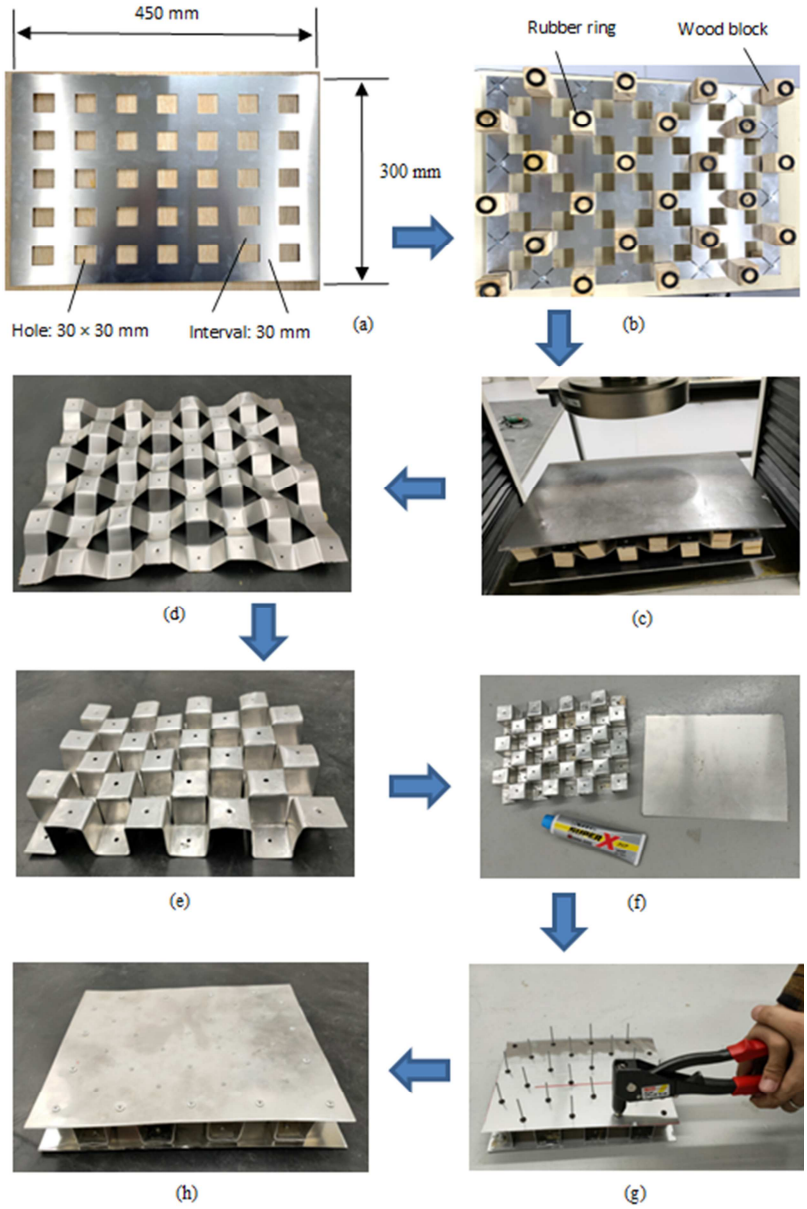

Figure 5. *Manufacturing flow of experimental aluminum cubic core panel.*

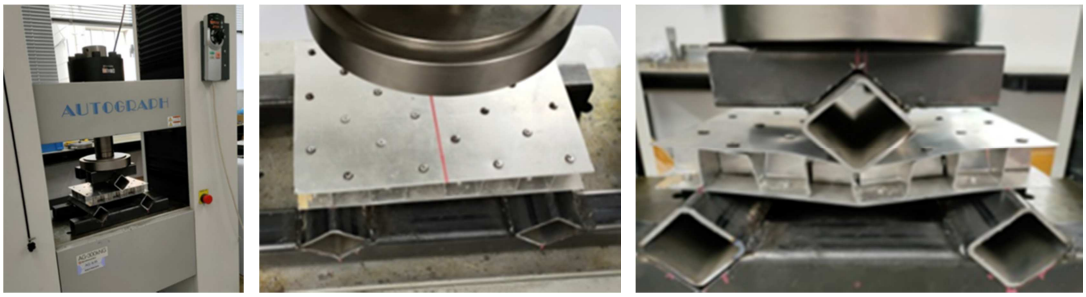

Figure 6. *Three-point bending test of manufactured cubic core panel.*

3. Results and Discussion

3.1. Examination by Three-Point Bending Test

To examine the mechanical properties of the cubic core panel manufactured in the previous section, a three-point bending test was performed, as shown in Figure 6. A Shimadzu AG-300kNG autograph machine was used. The support width of the three-point bending test was 200 mm. The curvature radius of the corner part of the three-point

bending jig that contacted the cubic core panel was 10 mm. The loading speed was 3 mm/m, and the maximum displacement was 20 mm.

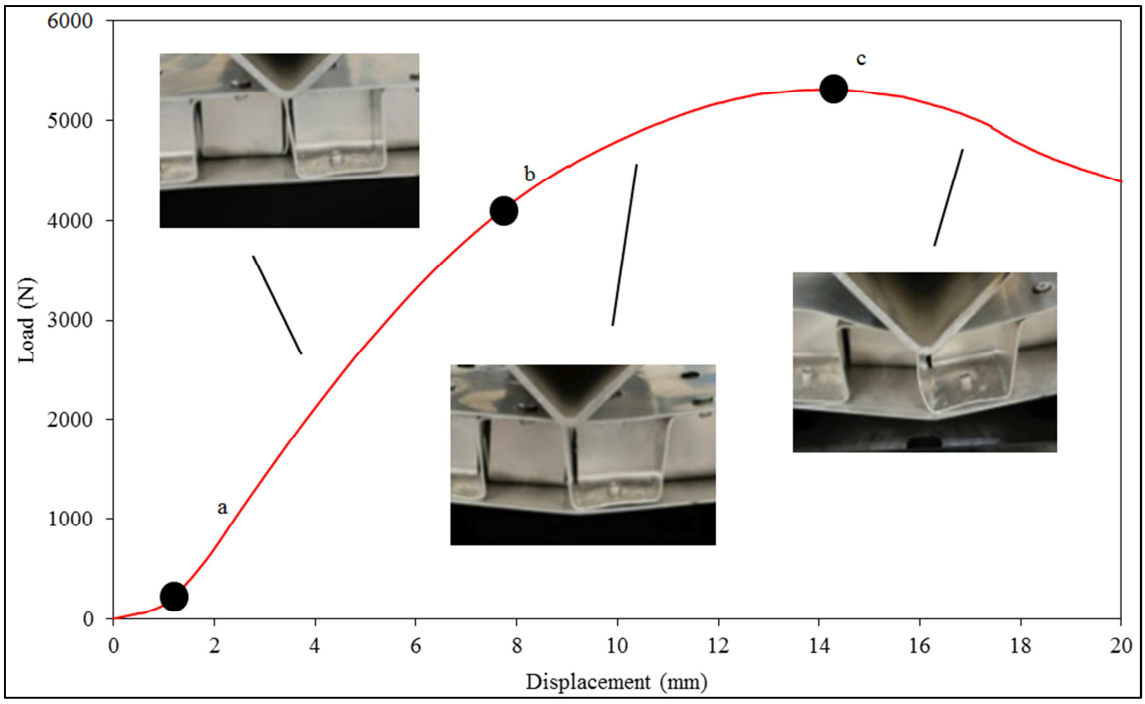

Figure 7. *Load–displacement results of three-point bending test of manufactured cubic core panels.*

Figure 7 shows the measurement results obtained from the three-point bending test. The load–displacement graph of the cubic core panel progresses in three steps.

First, in the initial stage of applying pressure, the jig and test piece slide sideways, and a phenomenon in which a slightly low load continues from the origin to point a can be observed. After passing point a, the graph between a and b becomes a straight line, indicating a linear relationship between the load and displacement. Its elastic modulus is 560 N/mm, and its linear elastic limit load value is approximately 4200 N.

Next, there is a slight curvature between b and c, and a nonlinear relationship exists between the load and displacement. However, the resistance to bending deformation continues to the maximum load point c while changing slowly, and the maximum load value is 5312 N.

Finally, after the maximum load point c has been exceeded, local buckling deformation occurs in the inner core material. Thus, the load continued to deform while it gradually decreased.

Two different cubic core panels were fabricated to investigate the effect of glue strength between the face plate and the core material. One was fixed only with rivets without using glue, as shown in Figure 8 (a). The other sheet was fixed using glue and rivets, as shown in Figure 8 (b). A three-point bending test was performed on each of the two cubic core panels. The measurement results are shown in Figure 9.

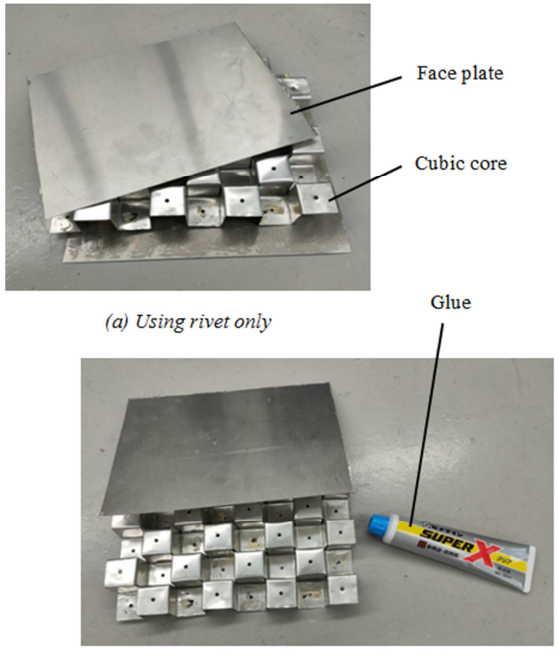

Figure 8. *Two methods of assemble flat face plate and cubic core.*

In Figure 9, the black line represents the measurement results when fixed with rivets and glue, and the blue line represents the measurement results when fixed with rivets only.

First, in the first elastic deformation process, the modulus of elasticity when fixed with rivets and glue was 560 N/mm, but when fixed with rivets alone, it was 525 N/mm, approximately

6.25% smaller. The elastic limit load when fixed with rivets and glue was 4200 N, and when fixed with rivets only, it was 2258 N, which is approximately 42.24% smaller. This shows that the elastic modulus and linear elastic limit load value are increased by using glue.

Next, after the load exceeded the elastic limit load, the cubic core panel fixed only with rivets broke owing to the stress concentration at the fixed part of the rivets, and the load value dropped sharply in the load–displacement graph. However, when the panel was fixed with rivets and glue, there was no partial breakage of the rivets, and the load value did not drop sharply in the load–displacement graph. The maximum load value was 3082 N when fixed with rivets alone and 5312 N when fixed with rivets and glue, which was approximately 41.98% smaller.

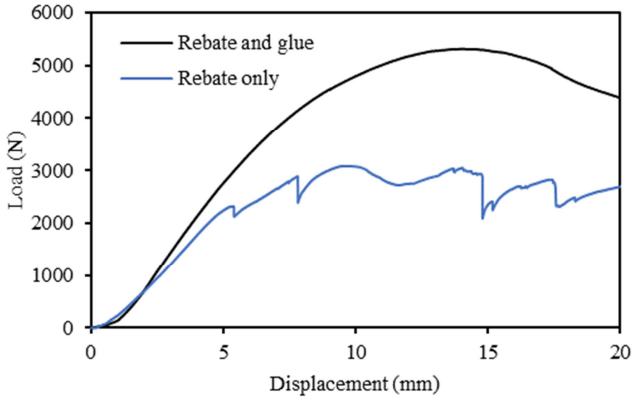

Figure 9. *Three-point bending test results for cubic core panels with different assembly methods.*

3.2. Comparison with Honeycomb Core Panel by FEM

Using the FEM analysis model shown in Figure 10, a static analysis of the cubic and honeycomb core panels was performed to compare the bending stiffness results of both.

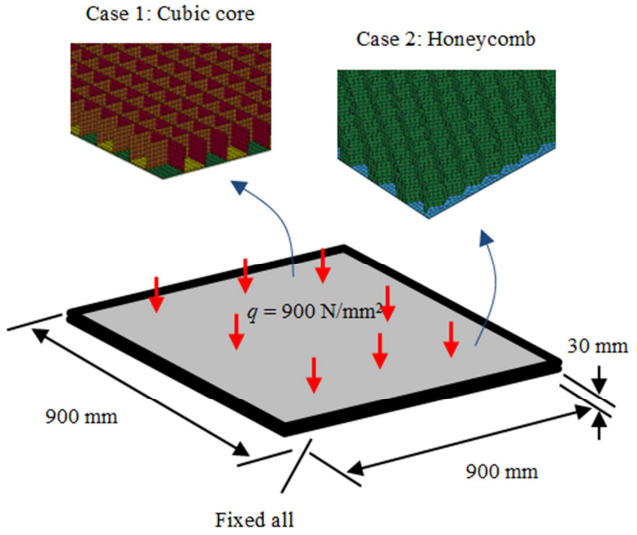

Figure 10. *FEM analysis model of uniformly distributed load on cubic core panel and honeycomb panel.*

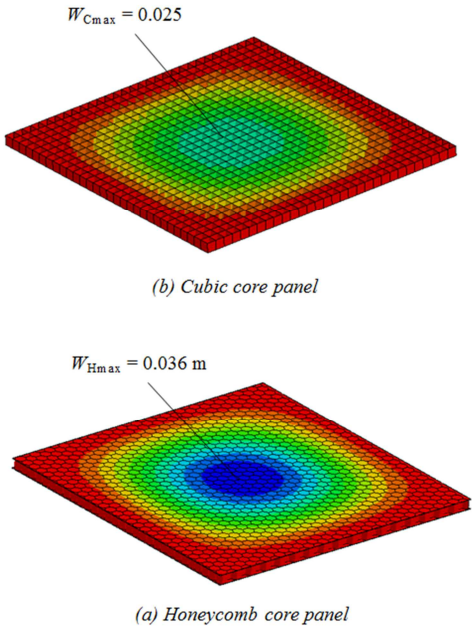

Figure 11. *Displacement distribution results of static FEM analysis.*

As shown in Figure 10, a uniformly distributed load was applied to a fixed square panel with a side length of 900 mm and a thickness of 30 mm. The core size of each panel was also 30 mm. The plate material used was aluminum A5052 with a Young's modulus of 72 MPa, Poisson's ratio of 0.33, and plate thickness of 0.8 mm. The average edge length of the analysis mesh was 5 mm. The cubic core panel was connected between the face plate and the core material under the rigid contact conditions of computer-aided engineering (CAE), and rivets were omitted.

Figure 11 (a) shows the static analysis results of the cubic core panel, and Figure 11 (b) shows the analysis results of the honeycomb panel. The maximum deflection of the cubic core panel was 0.025 m, and the maximum deflection of the honeycomb panel was 0.036 m.

To evaluate the bending stiffness of the lightweight panel, it is necessary to use the displacement value corresponding to the unit load.

The external load P can be calculated using the uniformly distributed load q and panel area A with the following equation.

$$P = qA = 1000 \times 0.9 \times 0.9 = 810 \text{ [N]} \quad (7)$$

Therefore, the stiffness of the cubic core panel and honeycomb panel can be evaluated by the following equations.

$$K_{cubic} = \frac{P}{W_{cubic}} = \frac{810}{0.025} = 32400 \text{ [N/m]} \quad (8)$$

$$K_{honey} = \frac{P}{W_{honey}} = \frac{810}{0.036} = 22500 \text{ [N/m]} \quad (9)$$

Using the material volume value calculated from the FEM analysis model and an aluminum plate density of 2700 kg/m^3, a cubic core panel weight of m_{cubic} = 9.72 kg and a honeycomb core panel weight of m_{honey} = 7.83 kg were obtained.

Therefore, the bending stiffness per unit weight can be evaluated by the following equations.

$$\bar{K}_{cubic} = \frac{K_{cubic}}{m_{cubic}} = \frac{324000}{9.72} = 3333.3 \text{ [N/kgm]} \quad (10)$$

$$\bar{K}_{honey} = \frac{K_{honey}}{m_{honey}} = \frac{22500}{7.83} = 2873.6 \text{ [N/kgm]} \quad (11)$$

Comparing Eqs. (10) and (11) reveals that, when the cubic core panel is used instead of the honeycomb core panel, the stiffness index per unit weight increases from 2873.6 to 3333.3 N/kgm (by 16.0%).

3.3. Application to Curved Corner Structure

In the actual structure, as shown in Figure 12, there are flat parts, such as the side walls and roof, and curved parts, such as the corner joints. In line with this, the cubic core panel proposed can be manufactured with a curved cubic core by partially applying a kirigami operation, as shown in Figure 13.

The actual manufacturing procedure is as follows. First, as shown in Figure 13 (a), the width of the curved part is determined according to the actual structural dimensions. Then, inside the curved corner, the shaded area in Figure 13 (b) is cut, and the panel is bent inward. As a result, curved cubic cores are obtained, as shown in Figures 13 (c) and (d). Finally, by fixing the bent face plate and cubic core to both sides of the curved cubic core using glue and rivets, a cubic core panel for curved corners, as shown in Figure 12, is obtained.

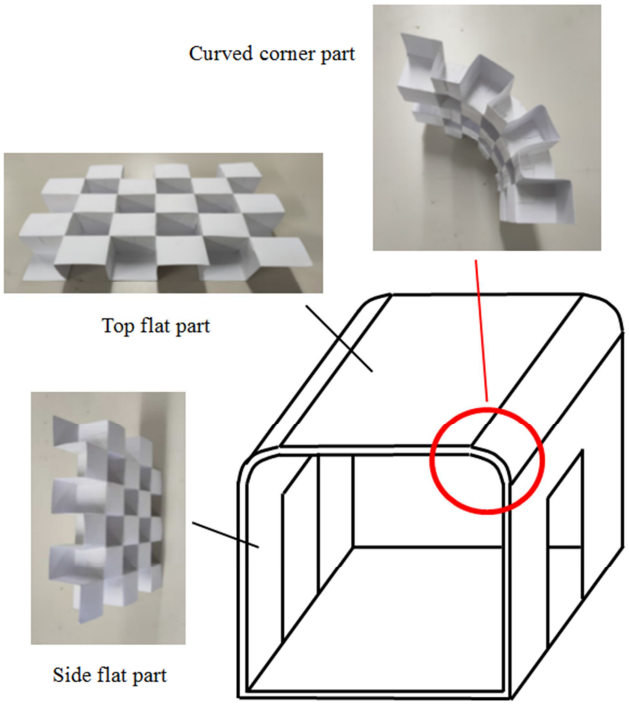

Figure 12. *The actual structure has flat part and a curved part.*

For practical use, it is important to determine the width of the curve and dimensions of the cutout portion appropriately for the cubic core.

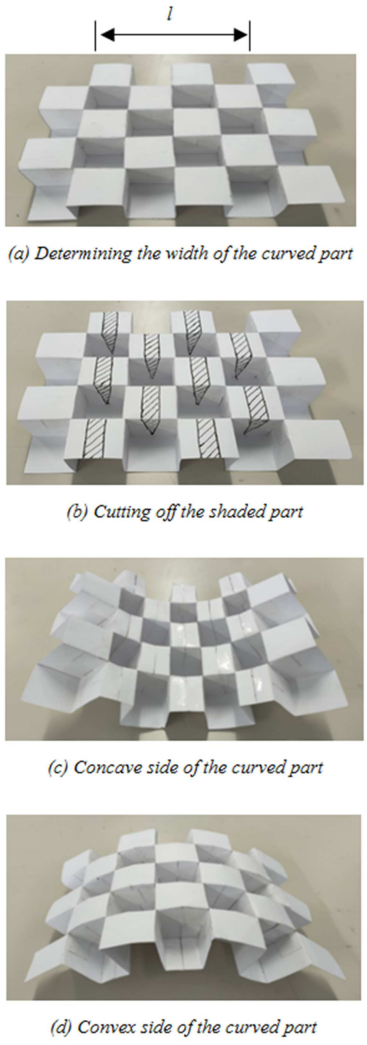

Figure 13. *Flowchart for manufacturing the partially curved part of cubic core panel.*

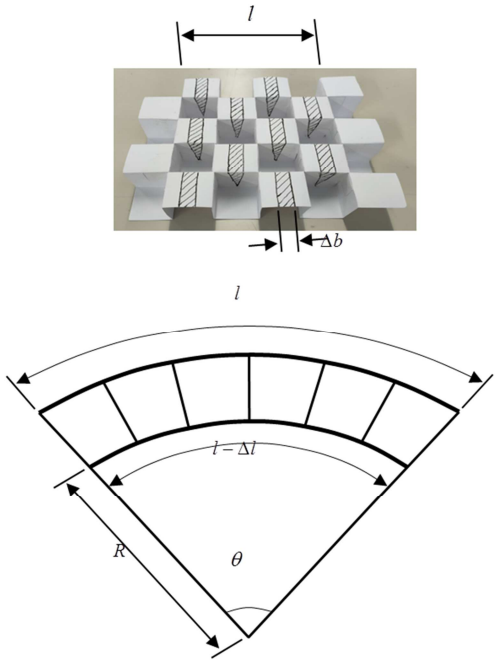

Figure 14. *Parameters of the curved part of the cubic core.*

Figure 14 shows the design parameters of the curved part of the cubic core. In Figure 14, l is the bending width, R is the radius of curvature of the inner surface of the curved part, and θ is the bending angle.

In the actual design, l, R and θ are given by the requirements of the curved structure. To manufacture the curved part accurately according to the designed dimensional requirements, it is necessary to determine appropriately the length Δl of the part to be cut and the width Δb to be cut from the cubic core on the inner surface.

According to Figure 14, the following relationship exists between the design parameters of the curved part.

$$\Delta l = l - R\theta \tag{12}$$

$$\Delta b = \frac{\Delta l}{n} = \frac{l - R\theta}{n} \tag{13}$$

where n is the number of cubic cores used to cut the material inside the bend. Equation (13) is the design equation for the curved part of the cubic core panel. The width Δb can be calculated by substituting the actual bending dimensions l, R, and θ into Equation (13).

3.4. Mass Manufacturing System Design

As shown in Figure 4, a prototype cubic core panel was manufactured using a simple pressing method with a wooden block and rubber ring to examine the performance. However, it is necessary to develop a more precise manufacturing method for practical applications.

In the forming process of the cubic core, the flat plate is bent vertically and simultaneously shrinks horizontally. Therefore, a four-bar link mechanism is proposed that connects adjacent bending blocks with parallel links (Figure 15).

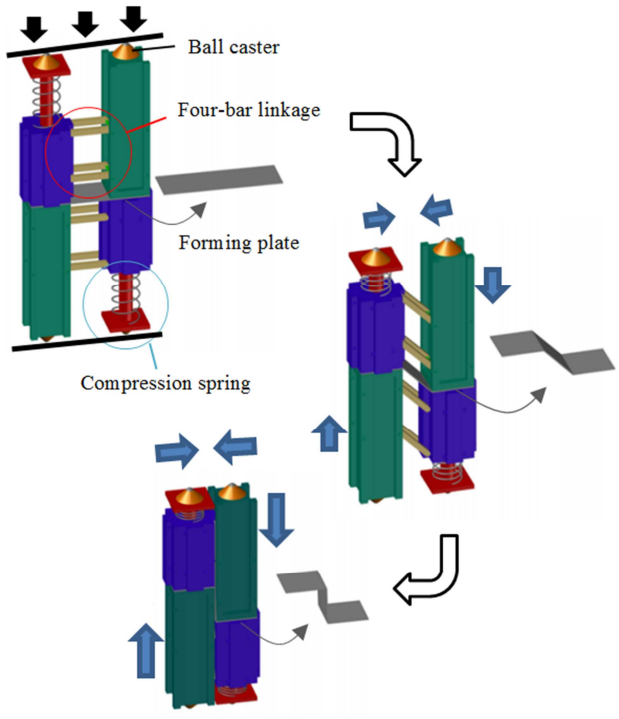

Figure 15. *Manufactured cubic core with two bending blocks.*

As shown in Figure 15, to perform bending, the forming plate is sandwiched between the upper and lower forming blocks, and pressure is applied in the vertical direction. An elastic spring attached to one end of the forming block is compressed, and the parallel movement of the four-bar linkage mechanism allows the adjacent forming blocks to shift vertically and move closer to each other in the horizontal direction. According to the order shown in Figure 15, the formed plate is bent up to a right angle. A ball caster is attached to the end face of the bending block so that the bending block slides easily in the horizontal direction.

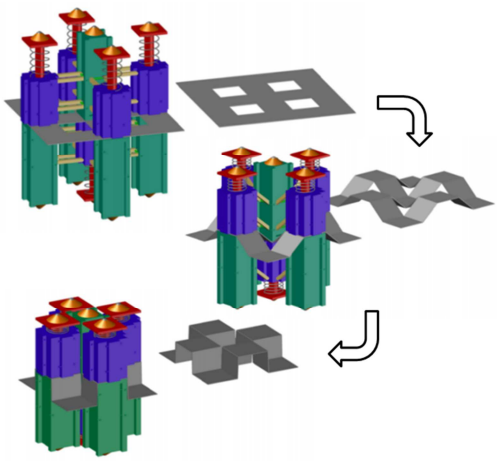

Figure 16. *Manufactured cubic core with five bending blocks.*

As shown in Figure 16, the forming block is expanded to five pieces, and pressure is applied in the vertical direction. The central bending block moves downward, whereas the four surrounding bending blocks move upward. Five cubic cores can be bent in the order shown in Figure 16.

According to the actual processing dimensions, multiple bending blocks can be connected in the horizontal direction to configure one dedicated processing die set, as shown in Figure 17. When applying pressure in the vertical direction, multiple cubic cores can be bent in one process according to the order shown in Figure 17.

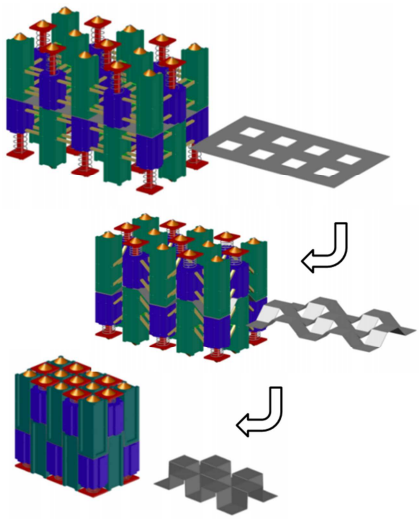

Figure 17. *Manufactured cubic core with multiple bending blocks.*

To study the bending load, Figure 18 shows the load condition of the bending part of the plate material. Here, P is the bending load, P_s is the reaction force of the compression spring, r is the curvature radius of the local bending, b is the side length of the cubic core, t is the plate thickness, and x is the bending displacement.

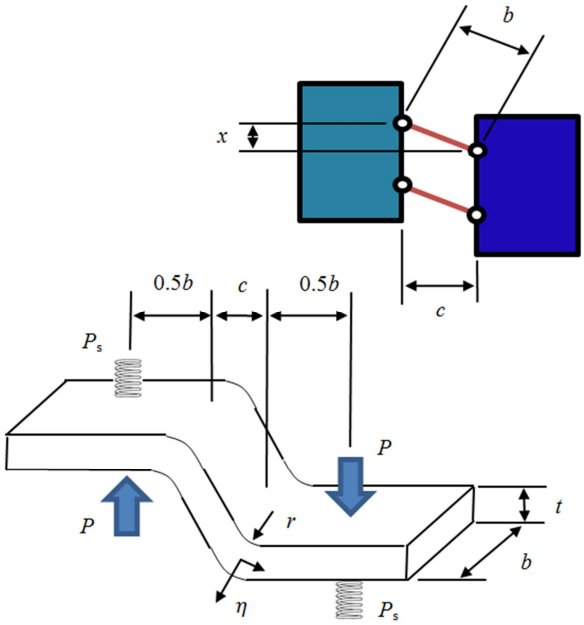

Figure 18. *Diagram of load parameters of the bending plate.*

The distance between adjacent blocks during forming and the reaction force of the elastic spring can be calculated using the following equations.

$$c = \sqrt{b^2 - x^2} \tag{14}$$

$$P_s = Kx \tag{15}$$

where K is the spring constant. Using the local coordinate η shown in Figure 18, the local bending moment is expressed by the following equation using stress σ.

$$\bar{M} = 2b \int_0^{\frac{t}{2}} \sigma \eta d\eta \tag{16}$$

The material properties of a plate are approximated by rigid plastic linear hardening, and the stress–strain relationship is expressed by

$$\sigma = \sigma_y + F\varepsilon \tag{17}$$

where σ_y is the yield stress, and F is the linear hardening factor. The strain can be calculated using the following equation.

$$\varepsilon = \frac{\eta}{r+\frac{t}{2}} = \frac{2\eta}{2r+t} \tag{18}$$

By substituting Equations (17) and (18) into Equation (16), the local bending moment can be expressed as

$$\bar{M} = \frac{\sigma_y bt^2}{4} + \frac{Fbt^3}{12r+6t} \tag{19}$$

According to Figure 18, the external force P - P_s intersecting in the vertical direction becomes a couple, and the bending moment is expressed by

$$M = (P - P_s)(b + c) \tag{20}$$

Using the equilibrium relationship between Equations (19) and (20), the following equation is obtained.

$$(P - P_s)(b + c) = \frac{\sigma_y bt^2}{2} + \frac{Fbt^3}{6r+3t} \tag{21}$$

By substituting Equations (14) and (15), the load required for bending is obtained as

$$P = Kx + \frac{\sigma_y bt^2}{2(b+\sqrt{b^2-x^2})} + \frac{Fbt^3}{(6r+3t)(b+\sqrt{b^2-x^2})} \tag{22}$$

The results were verified using the cubic core forming example in the previous section. The parameters of cubic core (side length b = 30 mm, aluminum plate yield stress σ_y= 215 MPa, work hardening factor F = 0, plate thickness t = 0.8 mm, and spring constant K = 0.15 N/mm) are substituted into Equation (22). As a result, the relationship between the load and displacement during molding is obtained (Figure 19).

As shown in Figure 19, the resistance to bending deformation increases gradually from the initial stage of forming, indicating that bending is relatively easy. However, after 80% bending, the forming load tends to increase as the relative distance between the forming blocks decreases.

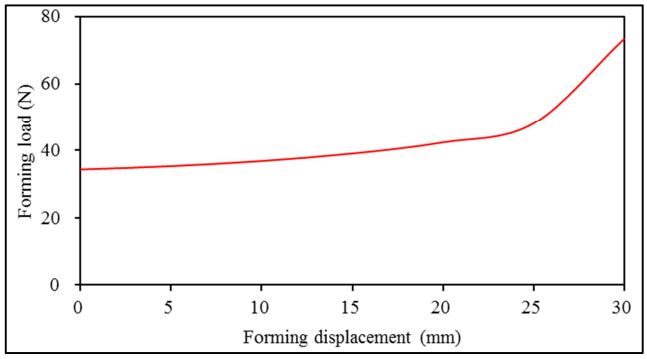

Figure 19. *Relationship between load and displacement during the cubic core bending formin.*

However, the results of Equation (22) and Figure 19 are the calculation results of the forming load required for bending one vertical wall. If the number of vertical walls of the cubic core panel to be processed is N, then the forming load required for processing is NP.

4. Conclusions

A cubic core lightweight panel was proposed, its mechanical properties and manufacturing methods were examined, and the following conclusions were obtained.

In the proposed cubic core panel, the square area of the bonding between the core material and the face plate is larger than that of the honeycomb core panel, and double bonding using glue and rivets is used; thus, the cubic core panel has a

stronger bonding strength than the honeycomb structure. In addition, the cubic core reinforced the face plate in a relatively thick manner. It was confirmed theoretically and by FEM analysis that the cubic core panel has a higher bending stiffness than the honeycomb panel under the same conditions.

For the investigation, a cubic core panel was manufactured using an aluminum plate, and the cubic core was processed by simple punching and bending. Cubic core panels were also easily assembled using glue and rivets. It was confirmed that the cubic core panel exhibited good manufacturing performance.

A three-point bending test was performed on the manufactured cubic core panel, and it was found that there are three stages in the relationship between the bending load and deformation. After the first stage with an initial linear relationship, the second stage with gradually nonlinear characteristics continues until the selected maximum load is reached. Finally, in the third stage, which begins after passing that load, the load value tends to drop gradually owing to local buckling. When a cubic core panel is used, it seems better to limit it to the first stage, which has a linear relationship.

According to the requirement for a lightweight structure with a curved portion, the curved portion of the cubic core panel can be manufactured by cutting part of the material from one side of the cubic core panel. A design equation for the curved portion of the cubic core panel was derived using the curvature radius and curvature angle of the actual curved structure.

A design for a cubic core forming system was studied for future practical development. By utilizing the parallel movement characteristics of the four-bar link mechanism, adjacent bending blocks can be shifted up and down. Simultaneously, they can gradually approach each other in the horizontal direction. Furthermore, equations for the bending load and displacement were derived, and important design factors for practical use were obtained.

References

[1] Czerwinski, F. (2021). Current Trends in Automotive Lightweighting Strategies and Materials. Materials, 14 (6631). doi.org/10.3390/ma14216631.

[2] Zhang, C., & Li, Z. (2022). A Review of Lightweight Design for Space Mirror Core Structure: Tradition and Future. Machines, 10 (1066). doi.org/10.3390/machines10111066.

[3] Möhring, H. C., Müller, M., Krieger, J., Multhof, J., Christian Plagge, C., Wit, J., & Misch, S. (2020). Intelligent lightweight structures for hybrid machine tools. Production Engineering, 14, 583. doi.org/10.1007/s11740-020-00988-3.

[4] Xiong, F., Wang, D., Ma, Z., Chen, S., Lv, T., & Lu, F. (2018). Structure-material integrated multi-objective lightweight design of the front end structure of automobile body. Structural and Multidisciplinary Optimization, 57, 829–847. doi: 10.1007/s00158-017-1778-1.

[5] Luo, W., Zheng, Z., Liu, F., Han, D., & Zhang. Y. (2020). Lightweight design of truck frame. Journal of Physics: Conference Series, 1653 (012063). doi: 10.1088/1742-6596/1653/1/012063.

[6] Tyflopoulos, E., & Steinert, M. (2020). Topology and Parametric Optimization-Based Design Processes for Lightweight Structures. Applied Sciences, 10 (4496). doi: 10.3390/app10134496.

[7] Yang, H., Brian, C. N., Yu, H. C., Liang, H. H., Chinee C. K. & Lai, F. W. (2022). Mechanical properties study on sandwich hybrid metal/ (carbon, glass) fiber reinforcement plastic composite sheet. Advanced Composites and Hybrid Materials, 5, 83-90. doi.org/10.1007/s42114-021-00213-4.

[8] Hammarberg, S., Kajberg, J., Larsson, S., & Jonsén, P. (2020). Ultra high strength steel sandwich for lightweight applications. SN Applied Sciences, 2 (1040). doi.org/10.1007/s42452-020-2773-5.

[9] Aggogeri, F., Borboni, A., Merlo, A., Pellegrini, N., & Ricatto, R. (2017). Vibration Damping Analysis of Lightweight. materials, 10 (297). doi: 10.3390/ma10030297.

[10] Liu, S., Zhang, B., Zhang, Yi, Z., Lai, X., & Yang, K. (2022). High Precision Manufacturing Technology of Complex Lightweight Integral Panel of Spacecraft. Journal of Physics: Conference Series, 2296 (012028). doi: 10.1088/1742-6596/2296/1/012028.

[11] Köksal, N. S., & Alkan, M. (2011). Stress Analysis in Al Based Composites Depending on Joining Quality. Mathematical and Computational Applications, 16 (1), 194-202. doi: 10.3390/mca16010194.

[12] Birman V., & Kardomateas, G. A. (2018). Review of current trends in research and applications of sandwich structures. Composites Part B, 142, 221–240. doi.org/10.1016/j.compositesb.2018.01.027.

[13] Saito, K., & Nojima, T. (2007). Development of Light-Weight Rigid Core Panels. Journal of Solid Mechanics and Materials Engineering, 1 (9), 1097–1104. doi: 10.1299/jmmp.1.1097.

[14] Li, Z., & Ma, J. (2020). Experimental Study on Mechanical Properties of the Sandwich Composite Structure Reinforced by Basalt Fiber and Nomex Honeycomb. Materials, 13 (1870), doi: 10.3390/ma13081870.

[15] Bourgeois, M. E., & Radford, D. W. (2022). Digital Manufacture of a Continuous Fiber Reinforced Thermoplastic Matrix Truss Core Structural Panel Using Off-the-Tool Consolidation. Journal of Composite Science, 6 (343). doi.org/10.3390/jcs6110343.

[16] Abhinav, S. N., & Budharaju, M. V. (2020). A Review Paper on Origin of Honeycomb Structure and its Sailing Properties. International Journal of Engineering Research & Technology, 9 (8), 861-866. doi: 10.17577/IJERTV9IS080336.

[17] Joshilkar, P., Deshpande, R. D., & Kulkarni, R. B. (2018). Analysis of Honeycomb Structure. International Journal for Research in Applied Science & Engineering Technology, 6 (5), 950–958. doi.org/10.22214/ijraset.2018.5153.

[18] Wang, B., A, P., Jiang, H., Zhang, Z., & Zhang, D. (2014). Honeycomb Structure Design Based on Finite Element Method. Applied Mechanics and Materials, 711 (2015), 74–77. doi: 10.4028/www.scientific.net/AMM.711.74.

[19] Arbintarso, E. S., Datama, H. F., Aviyanto, R. N. W., Prasetya, B., Purwokusumo, U. S. A. B., Aditiawan, B., Sangkoyo, P. P., & Adi, R. B. S. (2019). The Bending Stress on GFRP Honeycomb Sandwich Panel Structure for a Chassis Lightweight Vehicle. IOP Conf. Series: Materials Science and Engineering, 506 (012050). doi: 10.1088/1757-899X/506/1/012050.

[20] Zhang, Z., Chen, W., Gao, D., Xiao, L., & Han, L. (2020). Experimental Study on Dynamic Compression Mechanical Properties of Aluminum Honeycomb Structures. Applied Sciences, 10 (1188). doi: 10.3390/app10031188.

[21] Haq, A. U., Gunashekar, G., & Narala S. K. R. (2023). The Dynamic Response of AuxHex and Star-Reentrant Honeycomb Cored Sandwich Panels Subject to Blast Loading. Arabian Journal for Science and Engineering, 2023. doi.org/10.1007/s13369-022-07564-0.

[22] Mahamuni, P., Bhansali, B., Salunke, S., & Parikh, Y. (2015). A Study of Hypervelocity Impact on Honeycomb Structure. International Journal of Innovative Research in Science, Engineering and Technology, 4 (3), 921–925. doi: 10.15680/IJIRSET.2015.0403019.

[23] Chen, J. W., Liu, W., & Su X. Y. (2011). Vibration and Buckling of Truss Core Sandwich Plates on An Elastic Foundation Subjected to Biaxial In-plane Loads. Computers, Materials & Continua, 24 (2), 163–182. doi.org/10.3970/cmc.2011.024.163.

[24] Al-Shammari, M. A., & Al-Waily, M. (2018). Analytical investigation of buckling behavior of honeycombs sandwich combined plate structure. International Journal of Mechanical and Production Engineering Research and Development, 8 (4), 771–786. doi: 10.24247/ijmperdaug201883.

[25] Qiu, C., Guan, Z., Guo, X., & Li, Z. (2012). Buckling of honeycomb structures under out-of-plane loads. Journal of Sandwich Structures & Materials, 22 (3). doi.org/10.1177/1099636218774383.

[26] Wang, Z., Li, Z., Zhou, W., & Hui, D. (2018). On the influence of structural defects for honeycomb structure. Composites Part B, 142, 183–192. doi.org/10.1016/j.compositesb.2018.01.015.

[27] Chen, D. H., & Ozaki, S. (2009). Stress concentration due to defects in a honeycomb structure. Composite Structures, 89, 52–59. doi: 10.1016/j.compstruct.2008.06.010.

[28] Ouyang, S., Deng, Z., & Hou, X. (2018). Stress concentration in octagonal honeycombs due to defects. Composite Structures, 204, 814–821. doi.org/10.1016/j.compstruct.2018.07.087.

[29] Tokura, S., & Hagiwara, I. (2011). Shape Optimization to Improve Impact Energy Absorption Ability of Truss Core Panel. Journal of Computational Science and Technology, 5 (1). doi.org/10.1299/jcst.5.1.

[30] Sudarshan, G. (2018). Structural Optimization of Automobile Bumper Using Honeycomb Structure. International Journal of Science and Research, 7 (8). doi: 10.21275/ART2019695.

[31] Wang, L., & Saito, K. (2021). Honeycomb structures manufactured by a new method and its failure analysis. Journal of Physics: Conference Series, 1733 (012003). doi: 10.1088/1742-6596/1733/1/012003.

[32] Saito, K., Pellegrino, K., & Nojima, T. (2014). Manufacture of Arbitrary Cross-Section Composite Honeycomb Cores Based on Origami Techniques. Journal of Mechanical Design, 136 (051011). doi: 10.1115/1.4026824.

[33] Meloni, M., Cai, J., Zhang, Q., Lee, D. S, Li, M., Ma, R., Parashkevov, T. E., & Feng, J. (2021). Engineering Origami: A Comprehensive Review of Recent Applications, Design Methods, and Tools. Advanced Science, 8 (2000636). doi: 10.1002/advs.202000636.

[34] Park, J. J., Won, P., & Ko, S. H. (2019). A Review on Hierarchical Origami and Kirigami Structure for Engineering Applications. International Journal of Precision Engineering and Manufacturing-Green Technology, 6, 147–161. doi.org/10.1007/s40684-019-00027-2.